Materials Science & Engineering A 594 (2014) 235–245

Contents lists available at ScienceDirect

Materials Science & Engineering A

journal homepage: www.elsevier.com/locate/msea

Effects of aluminum content and strain rate on strain hardening behavior of cast magnesium alloys during compression

N. Tahreen [a], D.L. Chen [a,*], M. Nouri [b], D.Y. Li [b]

[a] Department of Mechanical and Industrial Engineering, Ryerson University, 350 Victoria Street, Toronto, Ontario M5B 2K3, Canada
[b] Department of Chemical and Materials Engineering, University of Alberta, 9107-116 Street, Edmonton, Alberta T6G 2V4, Canada

ARTICLE INFO

Article history:
Received 13 October 2013
Received in revised form
23 November 2013
Accepted 25 November 2013
Available online 2 December 2013

Keywords:
Magnesium alloy
Strain hardening
Aluminum effect
Strain rate sensitivity

ABSTRACT

The aim of this study was to identify the effects of aluminum content and strain rate on the compressive strain hardening behavior of AZ31, AZ61 and AZ91D cast magnesium alloys. The yield strength (YS) and ultimate compressive strength (UCS) of the alloys increased but the strain to failure decreased with increasing aluminum content, due to the presence of an increasing number of β-$Mg_{17}Al_{12}$ particles. The YS increased slightly with increasing strain rate, while the strain-rate dependence of the UCS and the strain to failure was basically absent, leading to a decreasing hardening capacity. The strain hardening exponent and strength coefficient evaluated via four equations of Ludwik, Hollomon, Swift, and Afrin et al. showed a similar increase with increasing strain rate in the AZ31 alloy, but were nearly independent of strain rate in the AZ61 and AZ91D alloys. The strength coefficient increased with increasing aluminum content based on all the four equations. The three alloys exhibited stage III hardening followed by stage IV hardening. AZ31 alloy had the longest stage IV hardening and the highest strain to failure, followed by AZ61 and AZ91D alloys.

1. Introduction

Lightweighting of materials and structures is being considered as one of key strategies for reducing the fossil fuel consumption and lowering anthropogenic climate-changing and environment-damaging emissions [1–6]. It has been reported that the fuel efficiency of ground vehicles can be improved by 6–8% for each 10% reduction in weight [7]. Magnesium alloys, as a category of ultra-lightweight metallic structural materials, have thus attracted a considerable interest in the transportation sectors in recent years, due to their high specific strength and stiffness, excellent damping capacity, superior castability, and machinability [8–19]. Currently, cast magnesium alloys are more widely used than wrought magnesium alloys because of their economic advantage for mass production of components due to lower processing and assembly costs and also for their isotropy in mechanical properties [20–22]. There have been many studies on the microstructure and tensile properties of various cast materials, e.g., [23–26]. However, little information is available about the compressive properties of cast magnesium alloys, while several studies on the compressive deformation behavior of extruded magnesium alloys have been reported, aiming to study the texture change and twin formation [27–31].

The mechanical properties of cast Mg alloys largely depend on alloy composition, microstructure, and texture [32]. It has been reported that for high pressure die cast magnesium alloys, the strain rate sensitivity (SRS) decreased as Al content increased [33,34]. For example, Song et al. [34] investigated three die cast magnesium alloys (AM20, AM50, and AM60) and observed that the strain rate sensitivity decreased with increasing Al content. Abbott et al. [35] showed that for die cast magnesium alloys (AS21, AM60, and AZ91, which contained 2%, 6%, and 9% Al, respectively), the strain rate sensitivity decreased with increasing Al content as well. However, Aune et al. [36] did not observe significant changes in the strain rate sensitivity within a strain rate range of 15–130 s^{-1} for AM50A, AM60B, and AZ91 die cast magnesium alloys. One possible reason could be that only higher Al contents ($>5\%$) would result in a lower strain rate sensitivity. Stanford et al. [37] examined the effect of Al solute on the strain rate sensitivity of Mg alloy and reported that the Mg–Al alloy exhibited a strain rate sensitivity being 30% lower than that of pure Mg. These studies suggest that the strain rate sensitivity of cast magnesium alloys strongly depends on the alloy composition. On the other hand, the strain hardening behavior of a material is an important aspect of deformation as a result of complex interactions among multiple factors, which include transitions from planar to cross dislocations slip, solid-solution alloying effects, precipitation effects and strain-induced phase transformations [38]. It is unclear how the Al content and the strain rate moderate the strain hardening behavior of cast magnesium alloys. The relationship

* Corresponding author. Tel.: +1 416 979 5000x6487; fax: +1 416 979 5265.
E-mail address: dchen@ryerson.ca (D.L. Chen).

0921-5093/$ - see front matter © 2013 Elsevier B.V. All rights reserved.
http://dx.doi.org/10.1016/j.msea.2013.11.078

among the alloy content, strain rate, strain hardening parameters and texture intensity deserves a detailed investigation. The aim of this study was, therefore, to identify the effects of aluminum content and strain rate on the strain hardening behavior and strain rate sensitivity of AZ31, AZ61, and AZ91D cast magnesium alloys, which contain 3, 6 and 9 wt% Al, respectively. Special attention was paid to the twin formation with varying aluminum contents.

2. Experimental method

Three Mg–Al–Zn (AZ series) cast alloys, AZ31, AZ61, and AZ91D, were used in the present study, which contained 3, 6, and 9 wt% Al, respectively, with ~1 wt% Zn and 0.15–0.50 wt% Mn. Cylindrical specimens with a diameter of 5 mm and height of 8 mm were machined and compression tests were performed until failure using a computerized Instron machine. The tests were carried out at room temperature and at a strain rate of $1\times10^{-4}\,s^{-1}$, $1\times10^{-3}\,s^{-1}$, $1\times10^{-2}\,s^{-1}$, $1\times10^{-1}\,s^{-1}$, respectively. In evaluating the stress–strain curves and strain hardening rates, the machine deformation was eliminated using a calibration curve to obtain the actual deformation of test samples. The compressive properties, including 0.2% yield strength (YS), ultimate compressive strength (UCS) and fracture strain (ε_f), were obtained based on the average values of two tests in each case. The deformed samples were cut along the compression axis using a slow diamond cutter and then cold mounted. The samples for microstructural examinations were ground with SiC abrasive papers up to a grit of #1200 and polished with diamond paste. Microstructures of both the base metal and deformed samples were observed via optical microscopy equipped with quantitative image analysis software after etching with an acetic picral solution containing 4.2 g picric acid, 10 ml acetic acid, 10 ml water, and 70 ml ethanol. The crystallographic texture of the materials was determined by a Panalytical X'Pert PRO X-ray diffractometer (XRD) using Cu K_α radiation (wavelength $\lambda=0.15406$ nm) at 45 kV and 40 mA with a sample tilt angle Ψ ranging from 0° to 70°. A set of five pole figures ({0001}, {10$\bar{1}$0}, {10$\bar{1}$1}, {11$\bar{2}$0}, and {10$\bar{1}$3}) were determined and analyzed using MTEX toolbox. Defocusing due to the rotation of sample holder was corrected using experimentally determined data obtained from the diffraction of magnesium powders received from Magnesium Elektron. The fracture surfaces were examined using a JEOL 6380LV scanning electron microscope (SEM) equipped with an Oxford energy dispersive X-ray spectroscopy (EDS) system and 3D fractographic analysis capacity.

3. Results and discussion

3.1. Microstructure and texture

Optical micrographs of AZ31, AZ61, and AZ91D cast alloys in the as-cast state are shown in Fig. 1. The microstructures of as-cast AZ31, AZ61, and AZ91D consisted of (a) equiaxed matrix, (b) network-like eutectic at the grain boundaries, and (c) round shaped particles as second phases in the matrix and also at the grain boundaries. The density of the second phase particles was the highest in AZ91D, followed by AZ61 and then AZ31. A small quantity of Al–Mn rich particles was also present in the cast magnesium alloys, as indicated in Fig. 2(a). This was revealed via an EDS analysis of AZ91D alloy shown in Fig. 2(b) where the eutectic network containing β-$Mg_{17}Al_{12}$ particles and Al–Mn rich white particles were clearly seen.

Fig. 3 shows the (0001) pole figures of AZ31, AZ61, and AZ91D cast alloys with a maximum (0001) pole intensity of 3.2, 3.2, and 5.2 MRD (multiples of a random density, or multiples of random distribution), respectively. Since the processing technology was casting, only relatively weak textures were observed, which indicates that the orientation of hcp unit cells inside the materials was fairly random. However, in comparison with AZ31 and AZ61 alloys, AZ91D alloy

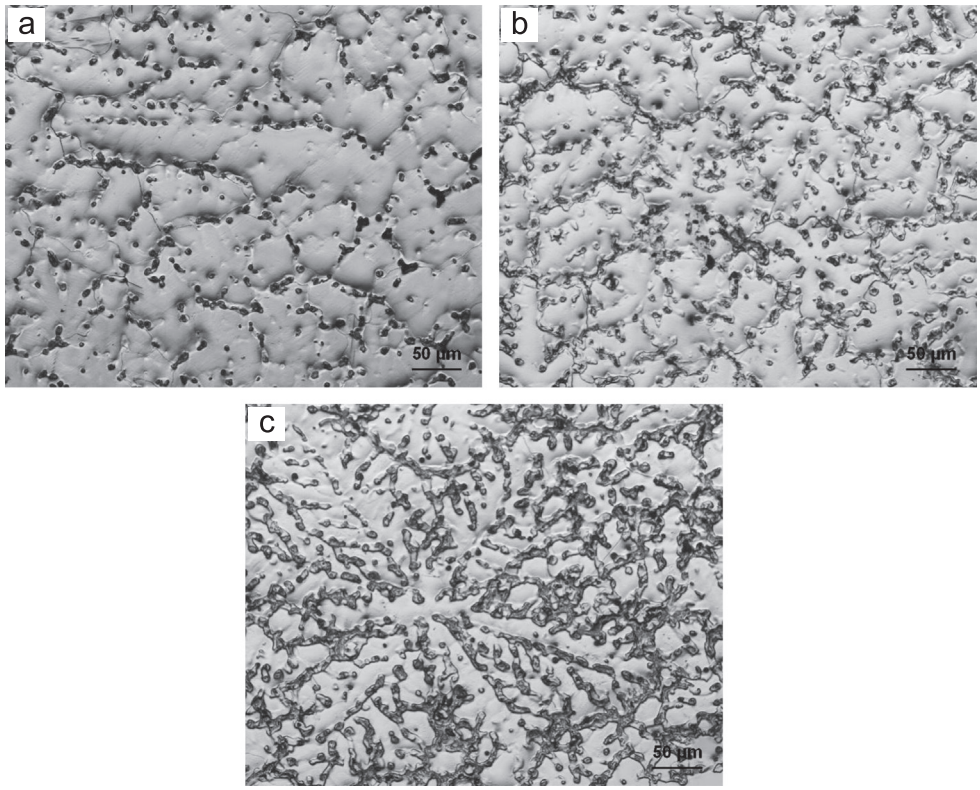

Fig. 1. Typical microstructures of cast Mg alloys in the as-cast condition (a) AZ31, (b) AZ61, and (c) AZ91D.